Study of the inhomogeneity of critical current under *in-situ* tensile stress for YBCO tape

Y P Zhu[1,2]**, W Chen**[1]**, H Y Zhang**[1]**, L Y Liu**[1]**, X F Pan**[3]**, X S Yang**[1] **and Y Zhao**[1]

[1] Key Laboratory of Magnetic Levitation Technologies and Maglev Trains (Ministry of Education), Superconductivity and New Energy R&D Center, Mail Stop 165#, Southwest Jiaotong University, Chengdu, 610031, People's Republic of China
[2] Southwestern Institute of Physics, Chengdu, 610041, People's Republic of China
[3] National Engineering Laboratory for Superconducting Materials (NELSM), Western Superconducting Technologies Co., Ltd., No.12 Mingguang Road, Xi'an, 710018, People's Republic of China

E-mail: xsyang@swjtu.edu.cn

Abstract

A Hall sensor system was used to measure the local critical current of YBCO tape with high spatial resolution under *in-situ* tensile stress. The hot spot generation and minimum quench energy of YBCO tape, which depended on the local critical current, was calculated through the thermoelectric coupling model. With the increase in tensile stress, the cracks which have different dimensions and critical current degradation arose more frequently and lowered the thermal stability of the YBCO tape.

Keywords: YBCO, inhomogeneity, critical current

(Some figures may appear in colour only in the online journal)

1. Introduction

The high critical current of REBCO (REBa$_2$Cu$_3$O$_x$, RE = rare earth elements) tape under high magnetic field makes it one of the most important alternatives that are used in the manufacture of high field magnets. Currently there are several high field superconducting magnet projects in the world [1–4]. However, the electrical properties of a coated conductor will be affected by bending strain, tensile stress and lamination stress in the manufacture and operation process of high temperature superconducting (HTS) coils, which may cause quench [5–7].

The distribution of I_c in coated conductors (CC) under radial strain and tensile stress is nonuniform, which is indicated by the hoop stress measurement of YBCO (YBa$_2$Cu$_3$O$_{7-\sigma}$) tape [8]. In the case of large hoop stress, a part of the tape showed plastic-like behavior, which caused local critical current degradation. Considering the extremely low normal zone propagation velocity for YBCO tape, which is only few centimeters per second, the heat spot generation

mostly generated in the degradation areas may lead to HTS coil burn. Therefore, the inhomogeneity of critical current is important in the simulation process of quench behavior for CC in aspects such as the estimation of device voltage and hot spot temperature for fault current limiter [9, 10], the predictor of critical current and n value for long length CC cable [11], and the determination of the time constant of the quench protection system for magnets [12].

Usually, the distribution of the I_c of CC is assumed to follow Gauss distribution, which may not reflect the real situation when CC is under tensile stress. Instead, the Weibull distribution is often used to simulate the critical current distribution of YBCO tape under strain [13]. The parameters of these two distributions is estimated from the measurement data. In the mechanical characteristic test of YBCO tape, the average I_c is usually measured by the four-probe method. The average I_c is accurate enough to evaluate the overall current-carrying performance. The local I_c degradation caused by cracks, however, is averaged due to the relative large resolution of the four-probe method, which is in the scale of
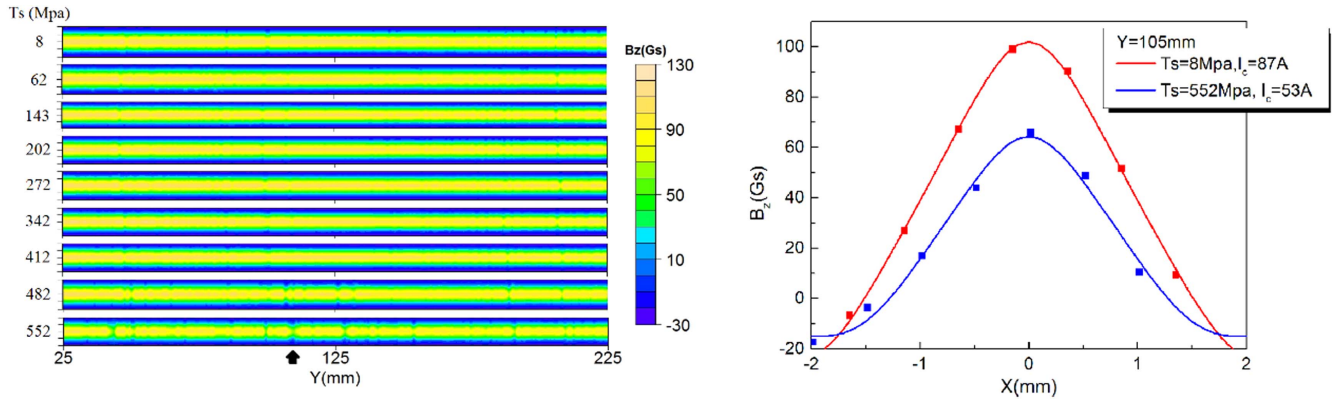
Figure 1. Measured distribution of the remanent field of YBCO tape at different tensile stress. T_s are from 8 Mpa to 552 Mpa. X and Y represent the axis along the tape width and length, respectively.

several centimeters. Another disadvantage of the four-probe method is that the average value of I_c seems too optimistic in the simulation process of heat spot generation [14]. Instead, using the non-destructive method to measure the I_c distribution in tensile stress, the scale of I_c distribution can be as small as a couple of millimeters not to mask the local phenomenon through averaging due to the high resolution of the non-destructive method.

The Hall sensor method is one of the most useful non-destructive methods [15]. The remanent or shielding field on the surface of the YBCO tape can be measured continuously by the Hall sensor and the local critical current is evaluated. The Hall sensor can also be used to study the I_c distribution of coated conductors *in-situ* applied magnetic field [16] or bending strain [17].

In this paper, we used Hall sensors to study the I_c distribution of YBCO tape under *in-situ* tensile stress, providing a more accurate way to measure the strain characteristic of CC than the four-probe method. Moreover, the measured I_c distribution under stress satisfied the demand for the modeling in which the discretization of the tape characteristics in the scale of the measured defects.

2. Experimental

A reel-to-reel Hall sensor system was built for evaluating the inhomogeneity of critical current of long HTS tape under *in-situ* tensile stress. The dialog of the system was shown in our previous work [18]. It was composed of a pay-off reel with a brake, a take-up reel with a motor, guide rollers, magnet, Hall sensors and a machine control system. The tensile stress applied in the CC was controlled by adjusting the current of the brake, which was proportional to the torque of the pay-off reel. The perpendicular component of the remanent field B_z around the CC tape was measured by a Hall sensor array after applying an external perpendicular magnetic field by a 0.2 T magnet in a liquid nitrogen bath. The Hall sensor array contained seven Hall sensors (AREPOC s.r.o, Slovakia). The effective area of each sensor was 50 μm $\times$ 50 μm, and the distance between each of Hall sensor was 0.5 mm. After

capturing the field mapping image of the CC in a measurement speed of 10 mm s^{-1} and the longitudinal resolution of 0.4 mm, the critical current was calculated by the least square fitting method according to the Bean critical state model [19, 20].

2 G HTS tapes SCS4050 produced by SuperPower, using ion-beam-assisted deposited MgO technology for the buffer layer and metal organic chemical vapor deposition for the superconducting layer, were measured in the experiment. The YBCO tape was initially wound into reels. Then the tensile stress was applied along the longitudinal direction of the YBCO tape by motor/brakes and the remanent field of the YBCO tape was measured by the Hall sensors at the same time. In order to easily measure the long tape in liquid nitrogen, a guide roller with the diameter of 100 mm was employed in the dewar. In this process, extra radial strain (ε_B) of about 0.05% was added to the superconducting layer. When the substrate faced the guide roller, extra tensile strain was added, but when the superconducting layer was facing the guide roller, the extra compress strain was applied. The YBCO tape was scanned by the Hall sensors under different tensile stress with extra tensile or compress strain. After the cracks were observed, the load was released and then the tape was retested.

3. Results and discussion

The remanent field of YBCO tape under the tensile stress (T_s) of 8 $\sim$ 552 Mpa with extra tensile strain of 0.05% is shown in figure 1. X and Y are the positions parallel to the sample width and length, respectively. In the images, when T_s is small, there is no obvious change in the remanent field. However, the remanent field is significantly distorted locally and the cracks arise frequently when the T_s is equal to 552 Mpa. Figure 1 shows that the lateral remanent field at X equals 105 mm when the T_s is 8 and 552 Mpa, respectively. The shape of the lateral field in the majority of damaged segments is symmetrical, thus the critical current is calculated by the least square method. As T_s increases from 8 Mpa to 552 Mpa, the remanent field reduces and I_c changes from
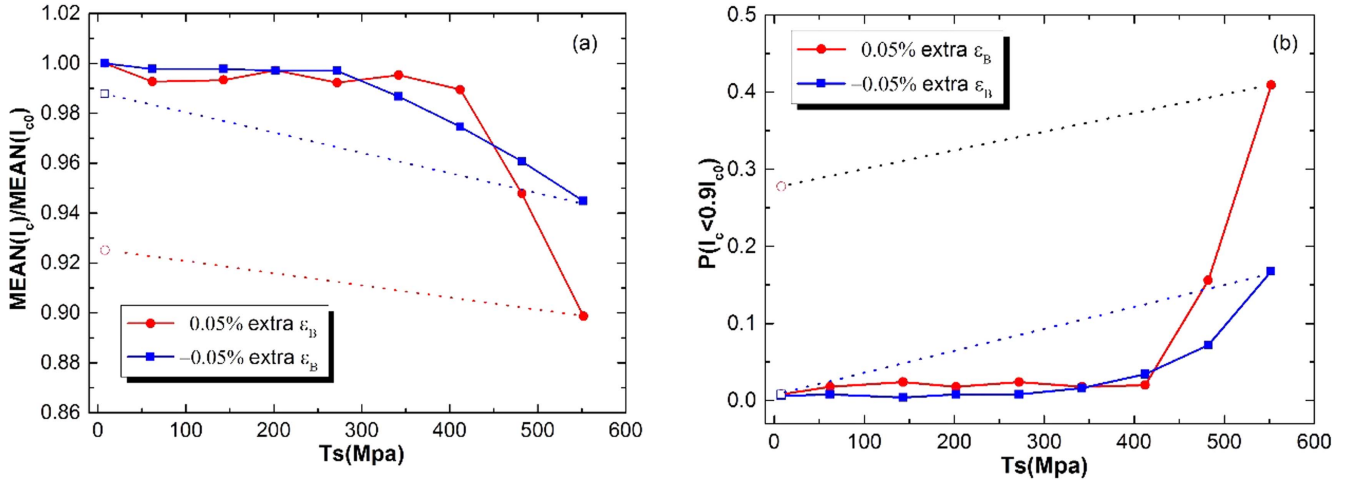
Figure 2. (a) Relative mean value of I_c and (b) crack exceedance probability of YBCO tape at various tensile stress. T_s are from 8 Mpa to 552 Mpa, while the extra $\varepsilon_B = 0.05\%$ and -0.05%, The solid and hollow points indicate the results measured when the load is applied and removed.

87 A to 53 A. This is because that segment of tape is partly damaged along the tape width by the maximum tensile stress of 552 Mpa. It is apparent that if the segment is totally damaged like a scratch along the tape width, the lateral field curve will not be symmetrical, and the freeze current along the tape width must be considered [21].

The statistical results of I_c which contain the relative mean value and crack exceedance probability are shown in figure 2. The relative mean value of I_c is defined as MEAN(I_c) divided by MEAN(I_{c0}); the crack exceedance probability is defined as the probability of the I_c less than 90% of MEAN(I_{c0}). MEAN(I_c) is the mean value of I_c and MEAN(I_{c0}) is the mean value of I_c when the tape is first measured under the tensile stress of 8 Mpa. The recovered result is also shown. When the tape is under tensile stress with extra ε_B of -0.05, considering that the tape is compress wound on a wheel with radius 50 mm under hoop stress, the relative mean value of I_c is reduced to 0.95 as the T_s reaches 552 Mpa and recovers to 0.99 as the T_s is removed. Even though the value of the crack exceedance probability reaches 0.14 when T_s is 552 Mpa, it returns to nearly zero after the load is released. This result proves the non-existence of cracks under T_s of 552 Mpa. However, things are different when the tensile stress is applied with an extra ε_B of 0.05%. While the T_s reaches 552 Mpa, the relative mean value of I_c and the crack exceedance probability changes to 0.9 and 0.4 respectively, and recovers to 0.93 and 0.28 when the load is released, respectively. The tolerance is less than the value in the literature [22]. On the one hand, the measurement method is different. On the other hand, the extra ε_B provides more tensile stress in the superconducting layer, which may lead to a more significant defect. The effect of the defect on the stability of magnet will be discussed elsewhere.

The thermoelectric coupling model, which consists of a one-dimensional (1D) or three-dimensional model, is commonly used for heat spot simulation in the YBCO tape with defects. Because only the 1D distribution of I_c is provided, we adopt the 1D model in this work. For every I_c segment along
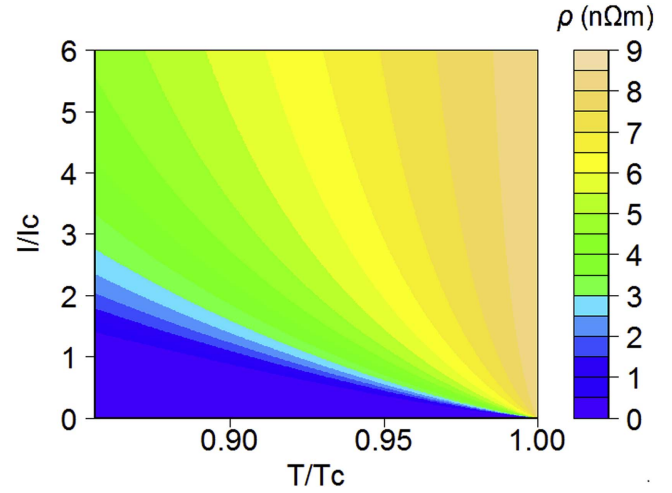

Figure 3. The resistivity of YBCO tape.

the tape length, we assume that the resistor of the segment consists of superconducting and non-superconducting parts in parallel. When the applied current is greater than I_c, the resistance of the superconducting part is assumed to follow the power law: $\rho(T) = E_c (J/J_c(T))^{n(T)-1}/J_c(T)$. The resistivity of the non-superconducting part is equal to the resistivity of the damaged YBCO tape, which is warmed to about 600 degrees to destroy its superconductivity [23]. The current sharing between two parts in every segment can be calculated using iteration algorithm [24]. The resistivity of YBCO tape is shown in figure 3. For most of the HTS pancake coil, whether it is insulated or not, the epoxy impregnation is used to solidify the coil. For the magnet with conduction or liquid cryogen cooling, the tape in the magnet is mainly in the adiabatic environment. The boundary condition is assumed adiabatic at 77 K. The temperature distribution of the tape is studied through the analytic solution of the one-dimension heat transfer model. Temperature varying thermal characteristics of the YBCO tape are taken from the literature [25].
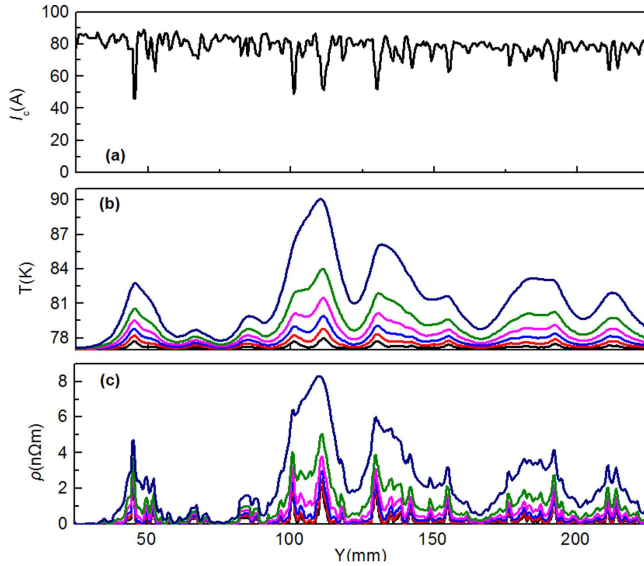
Figure 4. Critical current distribution (a), temperature profile (b) and equivalent resistivity profile (c) along the Y direction of YBCO tape under tensile stress of 552 Mpa, where the rated I_c is 87 A and the applied I is 95.7 A. The upper profile is for time equals 176 ms, the profiles below are for time equals 140, 112, 84, 56, and 28 ms, respectively.
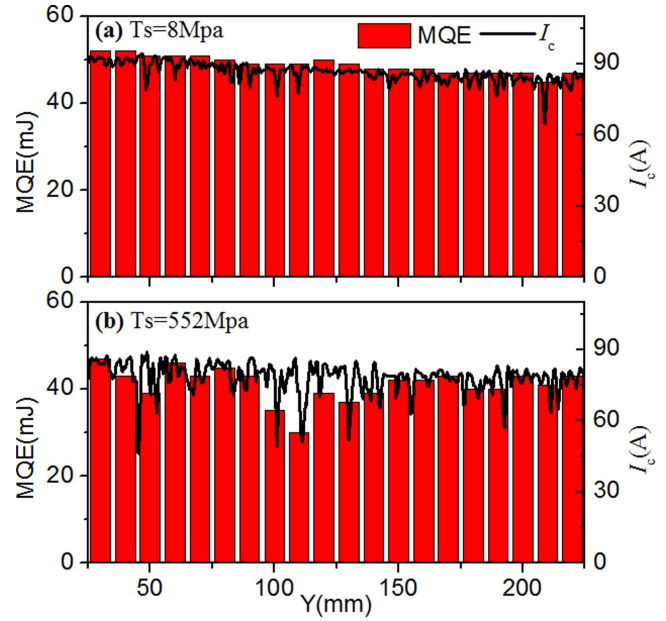

Figure 5. Critical current and MQE distribution for YBCO tape under tensile stress of 8 Mpa (a) and 552 Mpa (b) along the Y direction, where the rated I_c is 87 A and the applied I is 61 A.

Figure 4 shows a typical example of the temperature distribution along the tape length with defect. The tape is under tensile stress of 552 Mpa with extra ε_B of 0.5%. The applied current is 95.7 A, which is 1.1 times higher than the initial I_c. The adiabatic environment is 77 K. In the segment with a defect, the hot spot arises and reaches 90 K at 176 ms. For the tape under 8 Mpa in the same condition, the value is 411 ms. If the applied current is smaller than initial I_c, quench will occur more easily in the segment with a defect.

The distribution of minimum quench energy (MQE) is calculated. In every 10 mm segment, we apply a heat pulse to initiate a quench. The applied current in the tape is set to 0.7 times rated I_c to ensure that the tape will not quench without heat pulse in a relatively long time, like 10 s. The result is shown in figure 5. For comparison, the result of the initial tape is shown as well. The MQE scale of the initial tape is from 45 to 52 mJ, while for the tape under T_s of 552 Mpa, the minimum MQE is reduced to about 30 mJ, depending on the local I_c degradation. The results show that the cracks caused by tensile stress lead to more significant hotspots and the increase in heating power, which reduces the local MQE and lowers the thermal stability of the magnet.

It is clear that the non-destructive method has higher spatial resolution in the test of the critical current, compared with the four-probe method. But how does the I_c resolution affect the simulation of the hot spot? We try to illustrate this issue by simulation. From the power law equation, $V = E_c L(I/I_c)^{n-1}$, we can generate I_c series with different resolutions by changing the value of L. We convent the resolution of 0.4 mm, which is the real resolution in this work, into a lower resolution, like 2, 4, 8, 10 and 20 mm. The I_c distribution of tape under T_s of 552 Mpa with a resolution of 2, 10 and 20 mm is shown in figure 6. It is shown that the

higher the resolution, the lower the value of minimum local I_c. In order to evaluate the effect of I_c distribution with a different resolution, quantitative analysis is necessary. We defined T_{max} as the maximum temperature when V_{all} reaches 10 mV, which is a common threshold used in quench detection. V_{all} is the electrical voltage across the whole tape. The applied current is changed from 0.8 to 1.1 times rated I_c. It is shown that T_{max} at higher resolution is greater than that in lower resolution. From the point of the quench simulation of an HTS magnet, the hot spot temperature is the key factor. If the lower resolution of I_c is used, the calculated hot spot temperature may be too optimistic.

In the design and construction of the HTS magnet, since the HTS tape has its inhomogeneity, it is difficult to simulate an accurate I-V curve until the I_c distribution of the tape is measured. However, it is hard to test the I_c distribution in the real HTS magnet. Thus the statistical model is often used in the simulation. We compared the Gauss and Weibull models simulating the time the hottest point reaches 90 K. The Gauss random I_c distribution is created from the mean value and the standard deviation of measured I_c. The probability density function of the Weibull model is: $f(I_c) = m((I_c - I_{c,min})/I_0)^{m-1}\exp(-((I_c - I_{c,min})/I_0)^m)/I_0$. The three parameters of the Weibull model are estimated by least squares and linear approaches [26]. The values of m, I_0 and $I_{c,min}$, which represent shape, scale and location factor, are estimated as 11.323, 0.995 and 78.79, respectively. The relationship between the time the hottest point reaches 90 K and the applied current based on two different distribution of coated conductor while T_s is 552 Mpa is shown in figure 7. For each value of the applied current, 50 times simulation is performed and the mean value of the results is shown. The real distribution measured in this work is also included for comparison. In the simulation, the time of hottest point
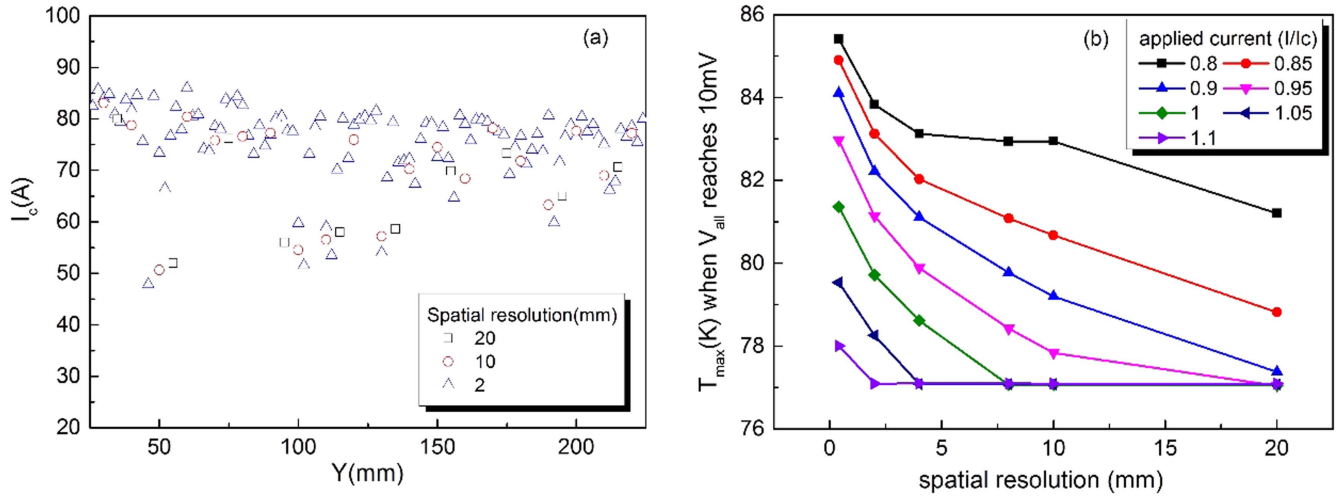
Figure 6. (a) Distribution of I_c under tensile stress of 552 Mpa with different spatial resolution. (b) T_{max} when V_{all} reaches 10 mV verses spatial resolution. Applied current is from 0.8 to 1.1 times rated I_c. The rated I_c is 87 A.

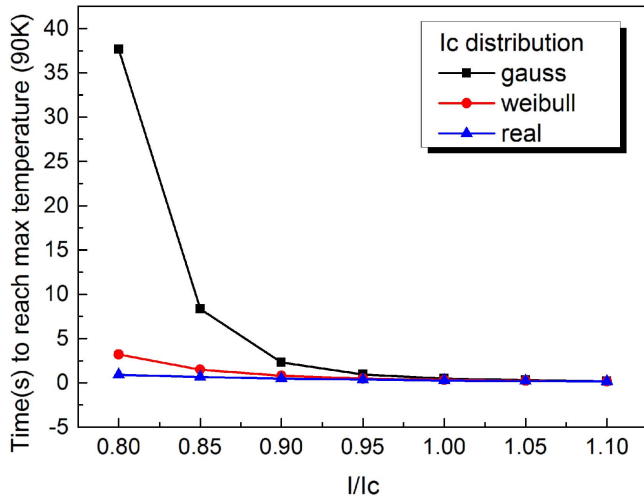**Figure 7.** Time to reach the T_{max}(90 K) at various applied currents based on three different distributions of coated conductor while T_s is 552 Mpa. The rated I_c is 87 A.
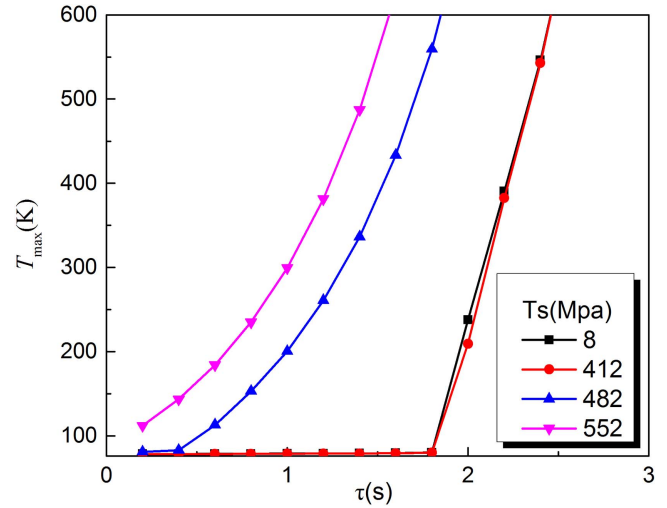

Figure 8. Maximum temperature T_{max} of hot spot versus time constant τ. The tensile stress is from 8 Mpa to 552 Mpa.

reaching 90 K calculated by real I_c distribution is smaller than that calculated by Gauss I_c distribution, especially while the applied current is smaller than the rated I_c. The simulation result showed that Weibull I_c distribution is more in accordance with actual circumstances than the Gauss one.

In the quench protection system of an HTS magnet, when a quench is detected, the power source is cut off as the dump resistor is connected to the coil. The power of the coil is fully dissipated in the dump resistor and the current flows in the coil can be described as $I = I_0 \exp(-t/\tau)$, where I_0 is initial applied current, τ is the time constant as $\tau = L/R$, R and L are the resistance and inductance of the dump resistor and coil, respectively. The optimized value of τ can be estimated from the simulation. For a different distribution of I_c under tensile stress with extra ε_B of 0.05%, the highest temperature of the hot spot at different τ is shown in figure 8. The environment is assumed adiabatic. The initial current is set as 1.1 times rated I_c. The time delay before the protection is initialed is set to 0.2 s. If the maximum allowable temperature of a ReBCO

tape is assumed to be 600 K, the maximum permissible time constant τ is reduced from 2.56 s for an initial tape to 1.5 s for the tape under tensile stress of 552 Mpa. Although the permissible τ mainly depends on the operation condition, the value of the resistance of the dump resistor can be selected as the maximum permissible value of τ is determined.

The YBCO magnet is able to operate beyond liquid helium temperature. It can be cooled by refrigeration rather than expensive liquid helium. Right now up to a 32 T immersion cooled HTS magnet has already been made and tested [27], however, the successful construction of a conduction cooled high field HTS magnet is still a challenge. If the cooling power is not enough, on the basis of the above analysis, the local area with a defect is easy to quench by a small thermal distribution. More detailed work on the inhomogeneity of critical current *in situ* is needed for further magnet design.

5

4. Conclusion

In conclusion, we have demonstrated a Hall sensor array system with high spatial resolution for evaluating the inhomogeneity of critical current of YBCO tape under *in-situ* tensile stress. The thermoelectric coupling model considering the measured critical current distribution under different tensile stress is performed. The results show that the crack caused by tensile stress in the superconducting layer will lead to more significant hotspots and reduce the minimum quench energy. The measured distribution of I_c under tensile stress is useful in thermoelectric modeling analysis for YBCO coils.

Acknowledgments

ORCID iDs

X S Yang ⓘ https://orcid.org/0000-0002-8686-9860

References

[1] Markiewicz W D *et al* 2012 *IEEE Trans. Appl. Supercond.* **22** 4300704
[2] Awaji S *et al* 2014 *IEEE Trans. Appl. Supercond.* **24** 4302005
[3] Wang Q *et al* 2013 *IEEE Trans. Appl. Supercond.* **23** 4300905
[4] Benkel T, Miyoshi Y, Escamez G, Gonzales D, Chaud X, Badel A and Tixador P 2016 *IEEE Trans. Appl. Supercond.* **26** 4302705
[5] Kataoka A, Tsukamoto O, Sekizawa S, Kawano Y, Kashima N, Nagaya S, Iijima Y and Saitoh T 2008 *IEEE Trans. Appl. Supercond.* **17** 3171
[6] Sugano M, Shikimachi K, Hirano N and Nagaya S 2007 *Physica* C **463** 742
[7] van der Laan D C, Ekin J W, Clickner C C and Stauffer T C 2007 *Supercond. Sci. Technol.* **20** 765
[8] Awaji S *et al* 2013 *IEEE Trans. Appl. Supercond.* **23** 4600305
[9] Colangelo D and Dutoit B 2012 *Supercond. Sci. Technol.* **25** 095005
[10] Mansour D A and Yehia D M 2013 *IEEE Trans. Appl. Supercond.* **23** 5602605
[11] Pothavajhala V, Kim C H, Graber L and Pamidi S 2015 *IEEE Trans. Appl. Supercond.* **25** 5400604
[12] Minagawa T, Fujimoto Y and Tsukamoto O 2013 *IEEE Trans. Appl. Supercond.* **23** 4702004
[13] Oh S, Kim H, Ha D, Ha H, Sim K, Dizon J and Shin H 2014 *IEEE Trans. Appl. Supercond.* **24** 6900204
[14] Badel A, Antognazza L, Therasse M, Abplanalp M, Schacherer C and Decroux M 2012 *Supercond. Sci. Technol.* **25** 095015
[15] Grimaldi G, Bauer M and Kinder H 2001 *Appl. Phys. Lett.* **79** 4390
[16] Shiohara K, Higashikawa K, Kawaguchi T, Inoue M, Kiss T, Yoshizumi M and Izumi T 2011 *Physica* C **471** 1041
[17] Rudnev I, Mareeva A, Mineev N, Pokrovskiy S and Sotnikova A 2014 *J. Phys.: Conf. Ser.* **507** 022029
[18] Zhu Y, Liu L, Wang G, Yang X and Zhao Y 2016 *IEEE Trans. Appl. Supercond.* **26** 8400304
[19] Bean C P 1962 *Phys. Rev. Lett.* **8** 250
[20] Bean C P 1964 *Rev. Mod. Phys.* **36** 31
[21] Higashikawa K, Inoue M, Kawaguchi T, Shiohara K, Imamura K, Kiss T, Iijima Y, Kakimoto K, Saitoh T and Izumi T 2011 *Physica* C **471** 1036–40
[22] Walsh R P, McRae D, Markiewicz W D, Lu J and Toplosky V J 2012 *IEEE Trans. Appl. Supercond.* **22** 8400406
[23] Young E A, Chappell S, Falorio I and Yang Y 2011 *IEEE Trans. Appl. Supercond.* **21** 3062–5
[24] Kiss T *et al* 2016 *Cryogenics* **80** 221–8
[25] Pelegrín J, Martínez E, Angurel L A, Xie Y and Selvamanickam V 2011 *IEEE Trans. Appl. Supercond.* **21** 3041
[26] Mbaruku A L and Schwarz J 2007 *J. Appl. Phys.* **101** 073913
[27] Kim K M, Bhattarai K R, Jang J Y, Hwang Y J, Kim K L, Yoon S, Lee S and Hahn S 2017 *Supercond. Sci. Technol.* **30** 065008